Electron-positron, parton-parton, and photon-photon production of τ-lepton pairs: Anomalous magnetic and electric dipole moments spin effects

Sw. Banerjee,[1] A. Yu. Korchin,[2,3,4] E. Richter-Was,[5] and Z. Was[4]

[1]*University of Louisville, Louisville, Kentucky 40292, USA*
[2]*NSC Kharkiv Institute of Physics and Technology, 61108 Kharkiv, Ukraine*
[3]*V.N. Karazin Kharkiv National University, 61022 Kharkiv, Ukraine*
[4]*Institute of Nuclear Physics Polish Academy of Sciences, PL-31342 Krakow, Poland*
[5]*Institute of Physics, Jagiellonian University, ul. Lojasiewicza 11, 30-348 Krakow, Poland*

(Received 12 July 2023; accepted 10 December 2023; published 16 January 2024)

Anomalous contributions to the electric and magnetic dipole moments of the τ lepton from new physics scenarios have brought renewed interest in the development of new charge-parity violating signatures in τ-pair production at Belle II energies, and also at higher energies of the Large Hadron Collider and the Future Circular Collider. In this paper, we discuss the effects of spin correlations, including transverse degrees of freedom, in the τ-pair production and decay. These studies include calculating analytical formulas, obtaining numerical results, and building semirealistic observables sensitive to the transverse spin correlations induced by the dipole moments of the τ lepton. The effects of such anomalous contributions to the dipole moments are introduced on top of precision simulations of $e^-e^+ \to \tau^-\tau^+$, $q\bar{q} \to \tau^-\tau^+$ and $\gamma\gamma \to \tau^-\tau^+$ processes, involving multibody final states. The τ decays are simulated along with radiative corrections, in particular electroweak box contributions of WW and ZZ exchanges are taken into account. Respective extensions of the Standard Model amplitudes and the reweighting algorithms are implemented into the KKMC Monte Carlo, which is used to simulate τ-pair production in e^-e^+ collisions, and the TauSpinner program, which is used to reweight events with τ pair produced in pp collisions.

DOI: 10.1103/PhysRevD.109.013002

I. INTRODUCTION

Electric and magnetic dipole moments of the τ lepton are sensitive to the violation of fundamental symmetries, such as the CP violation [1–3]. Recent measurements of dipole moments of the τ lepton at the Belle experiment [4], as well as observation of $\gamma\gamma \to \tau^-\tau^+$ production at the hadron colliders [5,6] have brought renewed interest in phenomena of electric and magnetic dipole moments of the τ lepton. Deviation of measured values of the magnetic moment of the muon [7] from predictions of the Standard Model (SM), and possibly enhanced contributions from new physics (NP) models to the magnetic moment of the τ lepton, makes these studies important and of contemporary interest. These NP contributions to magnetic moments are expected to be proportional to the square of the mass of the corresponding lepton. Several NP scenarios introduce dark weakly interacting scalars or vector states accompanying production of heavy fermions e.g. τ leptons. Such states and other new virtual particles via loop corrections, can be sources of anomalous contributions to the electric or magnetic dipole moments of the τ lepton, as mentioned in Refs. [8,9] and references therein.

The KKMC Monte Carlo (MC) has been used to generate events of the SM $e^-e^+ \to \tau^-\tau^+$ process for several decades, and is now enriched with several additional processes to describe NP effects potentially observable at e^-e^+ collider and the Belle II experiment [10]. In particular, recent development in Ref. [11] allows one to include anomalous contributions to electric and magnetic dipole moments of the τ lepton, in case of low-energy τ-pair production. In KKMC, all spin correlations are rigorously implemented, including quantum entanglement effects. This is the case for configurations where an arbitrary number of hard bremsstrahlung photons can be present. It can also provide valuable benchmarks for spin effects in $e^-e^+ \to \tau^-\tau^+$ process, with τ decays included.

The TauSpinner program is a convenient tool to study and prepare observables sensitive to the NP effects at hadron colliders. Its purpose is to introduce, with the help of weights, small effects on top of event samples of the SM content. It is imperative, as in case of KKMC, to evaluate if

TABLE I. Current status of predictions and measurements of anomalous magnetic (a), weak anomalous magnetic (a_w), electric (d) and weak electric (d_w) dipole moments/form factors, of the τ lepton, quoted at 95% confidence level.

	SM prediction	Experiment [20]
a	$1.17721(5) \times 10^{-3}$ [9]	$-0.052 < a < 0.013$ [21]
a_w	$-(2.10 + i0.61) \times 10^{-6}$ [22]	$\mathrm{Re}(a_w) < 1.14 \times 10^{-3}$ [23] $\mathrm{Im}(a_w) < 2.65 \times 10^{-3}$ at 95% CL [23]
d	-7.32×10^{-38} e cm [24]	$(-1.85 < \mathrm{Re}(d) < 0.61) \times 10^{-17}$ e cm [4] $(-1.03 < \mathrm{Im}(d) < 0.23) \times 10^{-17}$ e cm [4]
d_w	...	$\mathrm{Re}(d_w) < 5.01 \times 10^{-18}$ e cm [23] $\mathrm{Im}(d_w) < 11.15 \times 10^{-18}$ e cm [23]

the precision of the SM simulation is sufficient for the user's needs. Then, TauSpinner may be used to introduce NP and/or spin effects. The samples may be generated with the help of general purpose MC generators like PYTHIA [12], Sherpa [13] or with the help of other, sophisticated generator setup. In its earlier versions, TauSpinner was used to introduce the longitudinal spin effects, in the case of the Drell-Yan processes or the Higgs production with decays into τ leptons, at the LHC [14]. Later, they were extended to applications of the NP interactions [15] in the hard processes, in which lepton pairs are accompanied with one or two hard jets [15], and to include the transverse spin effects [16]. The list of applications was also extended to incorporate the electroweak (EW) effects [17,18].

Let us now introduce some terminology, which is used throughout the paper. In the reaction $\gamma\gamma \to \tau^-\tau^+$, where the τ lepton couples with on shell photons, we include the anomalous magnetic and electric dipole moments of the τ lepton. In the processes $e^-e^+ \to \tau^-\tau^+$ and $q\bar{q} \to \tau^-\tau^+$, where the couplings of the τ lepton with the photon or the Z-boson are virtual, one usually introduces form factors. For the photon exchange, we have form factors for the anomalous magnetic dipole moment (a) and the electric dipole moment (d), while for the Z-boson exchange, we have form factors for the anomalous weak-magnetic dipole moment (a_w) and the weak-electric dipole moment (d_w). In case of on shell photons with virtuality of $q^2 \sim 0$, the electromagnetic form factors reduce to the corresponding dipole moments. Similarly, for on shell Z-boson with virtuality $q^2 \sim M_Z^2$, the weak form factors reduce to the corresponding weak dipole moments (see, e.g. Ref. [19]).

All these form factors are connected to the chirality flipping operators. The terms proportional to electric and weak electric form factors are also CP violating. Anomalous magnetic form factor also receives a contribution from radiative corrections in the SM, which we separate from the NP term. As the electric dipole formfactor in the SM is highly suppressed, one can assume that this form factor comes exclusively from NP contributions.

The current experimental results and constraints for these dipole moments (or form factors in some cases), together with theoretical predictions in the SM, are presented in Table I.

In this paper, we focus on the effects of dipole moments/form factors on spin correlations in the τ-pair production and decay. Quantifying those effects requires explicit calculation of the matrix elements including longitudinal and transverse spin components and their correlations.

First, we consider the SM case, because it determines the nature of interfering contributions for analysis of anomalous dipole moments due to NP. The SM amplitude is evaluated in the improved Born approximation (IBA). The theoretical basis of IBA is formulated in Ref. [25], and our approach is explained in Ref. [17]. It allows us to separate the EW correction into pure QED part and the remaining one, sometimes called the genuine weak part. However, we shorten the name to simply refer to this as the EW correction. Numerically these corrections are included in IBA and rely on the EW Dizet library [25], which is installed in KKMC. The EW corrections are introduced with form factor corrections to the SM couplings and propagators, which enter the IBA amplitude used for calculation of EW weights. They represent complete $\mathcal{O}(\alpha)$ EW corrections with QED contributions removed but augmented with carefully selected dominant higher-order terms. The WW and ZZ box-diagram contributions, which are numerically important above the WW and ZZ threshold, are thus accounted for. This approach was very successful in analyses of LEP I precision physics, and later extended for use in Tevatron and LHC precision physics.

In the second step, we consider the anomalous dipole moments themselves. These studies include calculation of the analytical formulas, validations of the tools, and an attempt to build semirealistic observables sensitive to transverse spin correlations induced by the dipole moments. Impact on the size of cross sections for τ-pair production is addressed marginally. Note, that effect of dipole moments in the radiative decay $Z \to \tau^-\tau^+\gamma$ based on LEP data was discussed in Ref. [26], and for $\gamma\gamma \to \tau^-\tau^+$ in peripheral Pb + Pb collisions in Ref. [27].

Technically, the effect of anomalous dipole moments can be introduced on top of precision simulations of $e^-e^+ \to$

$\tau^-\tau^+$, $q\bar{q} \to \tau^-\tau^+$ and $\gamma\gamma \to \tau^-\tau^+$ processes, involving multibody final states and correlations between τ decay products. The MC techniques using event-by-event weights, are convenient for this purpose. The KKMC MC is used for simulating spin-correlation effects in τ pair produced in e^-e^+ collisions, while the TauSpinner program is used for reweighting events where τ pairs are produced in pp collisions.

Our paper is organized in the following manner. In Sec. II, we present analytic calculation of the spin correlation matrix, which include effects of the τ-lepton anomalous magnetic and electric dipole form factors. Analytic formulas, described in Sec. III, are useful for implementation of transverse spin correlations for each of the parton level processes $q\bar{q} \to \tau^-\tau^+$, $e^-e^+ \to \tau^-\tau^+$ and $\gamma\gamma \to \tau^-\tau^+$. In Sec. IV, we recall main points of the KKMC and TauSpinner reweighting algorithms for inclusion of the dipole moments. Discussions on the possible test observables and some numerical results are collected in Sec. V. Section VI closes the paper with a summary and outlook.

II. AMPLITUDES AND SPIN CORRELATIONS

In Ref. [11], formulas for including anomalous magnetic and electric dipole form factors in elementary $2 \to 2$ parton processes of τ-pair production were discussed. The elementary parton-level and improved Born-level formulas were presented there for $e^-e^+ \to \tau^-\tau^+$ process, including details of reference frames[1] used in spin-correlation matrix calculation. Those formulas are however limited to low energies, where contribution of Z-boson exchange can be neglected in specific applications.

For higher-energy $e^-e^+ \to \tau^-\tau^+$, and also for $q\bar{q} \to \tau^-\tau^+$ parton level processes at the LHC, inclusion of the contribution due to the exchange of Z-boson is necessary. For very high τ-pair virtuality of more than 160 GeV, the contributions from doubly resonant WW and ZZ boxes need to be taken into account as well, following for example, Refs. [17,28] on TauSpinner and KKMC, where EW loop corrections installation is documented. Here we extend results of Ref. [11], and derive the formulas including Z and γ^* exchanges and their interference.

[1]A comment on the direction of reference frames is in place here. Formally speaking, the interchange of reaction name between $e^-e^+ \to \tau^-\tau^+$ and $e^+e^- \to \tau^+\tau^-$ is purely conventional and not of physics content. The choice however does imply which among the incoming e^- or e^+ particle is taken as the first beam (analogously if τ^- or τ^+ is taken as the first outgoing lepton) in the positive $\hat{z}$ direction. The second choice was used in some of older projects. Nowadays, the choice of e^- is made more frequently, as the more energetic beam in asymmetric colliders. Due to overlapping conventions, a sign mismatch may occur. In our programs, a rotation by an angle of π around the $\hat{y}$ axis may be necessary before the anomalous contributions are inserted into the other parts of the code.

To complete the picture we also derive the formulas for $\gamma\gamma \to \tau^-\tau^+$ processes in the so-called light-by-light scattering approximation, which recently became of high interest in the analysis of heavy-ion beam collisions at the LHC [5,6].

Let us start by introducing formalism for $f_i\bar{f}_i \to \tau^-\tau^+$ process, where $i = e$, u, d or γ. For the $\gamma\gamma$ initial state, the symbol $\bar{f}_i$ refers to the second incoming photon. Thus, in our generalized notation, we consider

$$f_i(k_1) + \bar{f}_i(k_2) \to \tau^-(p_-) + \tau^+(p_+), \tag{1}$$

where the four-momenta satisfy the conservation relation: $k_1 + k_2 = p_- + p_+$.

In the center-of-mass (c.m.) frame, the components of the momenta are

$$\begin{aligned} &p_- = (E, \vec{p}), \;\; p_+ = (E, -\vec{p}), \;\; \vec{p} = (0, 0, p), \\ &k_1 = (E, \vec{k}), \;\; k_2 = (E, -\vec{k}), \;\; \vec{k} = (E\sin\theta, 0, E\cos\theta), \end{aligned} \tag{2}$$

so that the $\hat{z}$ axis is along the momentum $\vec{p}$, the reaction plane $\hat{x}\,\hat{z}$ is defined by the momenta $\vec{p}$ and $\vec{k}$, and the $\hat{y}$ axis is along $\vec{p} \times \vec{k}$. Here, $E = \sqrt{s}/2$, $p = \beta E$ is the τ-lepton three-momentum, $\beta = (1 - 4m_\tau^2/s)^{1/2}$ is the velocity, m_τ is the mass of the τ lepton and $s = (p_- + p_+)^2$. The mass of initial lepton or quark is neglected hereafter.

The quantization frames of τ^- and τ^+ are connected to this reaction frame by the appropriate boosts along the $\hat{z}$ direction. Note that the $\hat{z}$ axis is parallel to momentum of τ^- but antiparallel to momentum of τ^+. The beams momenta reside in the $\hat{x}\,\hat{z}$ plane. Only the reaction frame, the τ^- and the τ^+ rest frames are used for calculations throughout the paper. The vector indices used in the formulas: 1, 2, 3, 4 correspond to $\hat{x}, \hat{y}, \hat{z}, \hat{t}$ directions, respectively.

A. The $f_i\bar{f}_i \to \tau^-\tau^+$, $i = e$, u, d case

1. Dipole form factors and improved Born approximation

We consider the $\gamma\tau\tau$ electromagnetic vertex to have the following structure:

$$\Gamma^\mu_\gamma(q) = -ieQ_\tau\left\{\gamma^\mu + \frac{\sigma^{\mu\nu}q_\nu}{2m}[iA(s) + B(s)\gamma_5]\right\}, \tag{3}$$

where $\sigma^{\mu\nu} = \frac{i}{2}[\gamma^\mu, \gamma^\nu]$, e is the charge of the positron, Q_τ is the charge of τ lepton in units of e, $A(s) = F_2(q^2)$ is the Pauli form factor, and $B(s) = F_3(q^2)$ is the electric dipole form factor, which depend on $s = q^2$, where $q = k_1 + k_2 = p_- + p_+$. At the on shell photon point, $A(0)$ is an anomalous dipole moment a, while $B(0)$ is related to the CP violating electric dipole moment d,

$$A(0) = a = \frac{1}{2}(g-2), \qquad B(0) = \frac{2m_\tau}{eQ_\tau} d, \tag{4}$$

where g is the gyromagnetic factor.

To separate SM contribution from NP we explicitly include the QED correction to $A(s)$ in the first order in $\alpha = e^2/(4\pi)$ [29]

$$A(s)_{\rm QED} = \frac{\alpha m_\tau^2}{\pi s\beta}\left(\log\frac{1-\beta}{1+\beta} + i\pi\right). \tag{5}$$

Therefore, we have

$$A(s) = A(s)_{\rm QED} + A(s)_{NP}, \quad B(s) = B(s)_{NP}, \tag{6}$$

neglecting very small contribution to $B(s)$ in the SM.

The $Z\tau\tau$ vertex is chosen to have the following structure:

$$\Gamma_Z^\mu(q) = -i\frac{g_Z}{2}\left\{\gamma^\mu(v_\tau - \gamma_5 a_\tau) + \frac{\sigma^{\mu\nu}q_\nu}{2m}[iX(s) + Y(s)\gamma_5]\right\}, \tag{7}$$

where $g_Z = e/(s_W c_W) = 2M_Z(\sqrt{2}G_F)^{1/2}$, $s_W \equiv \sin\theta_W$, $c_W \equiv \cos\theta_W$; θ_W is the weak mixing angle and $G_F = 1.1663788(6)\times 10^{-5}$ GeV^{-2} [20] is the Fermi constant. The vector and axial-vector couplings for the τ lepton are $v_\tau = -1/2 + 2s_W^2$ and $a_\tau = -1/2$, respectively, $X(s)$ is the weak-anomalous magnetic form factor, and $Y(s)$ is related to the CP violating weak electric form factor.[2]

The $X(M_Z^2)$ was evaluated for the SM in Ref. [22]. Using this calculation, in our notation $X(M_Z^2)_{\rm SM} = -(2.10 + i0.61)\times 10^{-6}\times(2s_W c_W)$. It is rather small, and this contribution is not explicitly included in our code, as elaborated in Sec. IV, but can easily be included if necessary. In this description, only the anomalous component is included, but $X(M_Z^2)_{\rm SM}$ can be introduced into the code, as additional part of $X(M_Z^2)$.

For the initial state fermion f_i, the electric charge in unit of e is denoted as Q_i, while the vector and axial-vector constants are denoted by v_i and a_i, respectively, as shown in Table II.

To simplify calculations, it is convenient to use the Gordon identities for the matrix elements of $\Gamma_\gamma^\mu(q)$ and $\Gamma_Z^\mu(q)$. This allows one to rewrite the respective currents as

$$\bar u(p_-)\Gamma_\gamma^\mu(q)v(p_+) = -ieQ_\tau\bar u(p_-)\left\{\gamma^\mu(1+A(s)) + \frac{(p_+-p_-)^\mu}{2m}[A(s) - iB(s)\gamma_5]\right\}v(p_+), \tag{8}$$

[2]Sometimes these form factors are defined with the additional factor $(2c_W s_W)^{-1}$ [19,22,30].

TABLE II. Electric charge (in units of e), vector and axial-vector couplings for leptons, u and d quarks. The measured values of the effective couplings [20] are also shown under the values predicted by the SM. It is worthwhile to note the change of sign between the leptons and the u quark.

Fermion	Q_i	v_i	a_i
$e^-(\mu^-,\tau^-)$	-1	$-\frac{1}{2}+2s_W^2$	$-\frac{1}{2}$
		-0.03783 ± 0.00041	-0.50123 ± 0.00026
u	$+\frac{2}{3}$	$+\frac{1}{2}-\frac{4}{3}s_W^2$	$+\frac{1}{2}$
		$+0.266 \pm 0.034$	$+0.519^{+0.028}_{-0.038}$
d	$-\frac{1}{3}$	$-\frac{1}{2}+\frac{2}{3}s_W^2$	$-\frac{1}{2}$
		$-0.38^{+0.04}_{-0.05}$	$-0.527^{+0.040}_{-0.028}$

$$\bar u(p_-)\Gamma_Z^\mu(q)v(p_+) = -i\frac{g_Z}{2}\bar u(p_-)\left\{\gamma^\mu((v_\tau + X(s)) - \gamma_5 a_\tau) + \frac{(p_+-p_-)^\mu}{2m}[X(s) - iY(s)\gamma_5]\right\}v(p_+). \tag{9}$$

Next we introduce radiative corrections following Refs. [17,25]. The amplitude, called $\mathcal{M}^{\rm IBA}$, for arbitrary initial (i) and final (f) fermions can be written as

$$\mathcal{M}^{\rm IBA} = \frac{e^2 Q_f Q_i}{s} V_{fi}(s,t)\gamma_\mu \otimes \gamma^\mu + \left(\frac{g_Z}{2}\right)^2 \frac{Z_{fi}(s,t)}{d(s)}\gamma_\mu[v_i(s,t) - a_i\gamma_5] \otimes \gamma^\mu[v_f(s,t) - a_f\gamma_5], \tag{10}$$

where the following shortcut notation is used; operator on the left of $\otimes$ is sandwiched between the spinors $\bar v(k_2)\ldots u(k_1)$, and operator on the right of $\otimes$ is sandwiched between the spinors $\bar u(p_-)\ldots v(p_+)$. In Eq. (10) Q_i and Q_f are the charges of initial and final fermions in units of e.

Furthermore, $t = (k_1 - p_-)^2$, $d(s) = s - M_Z^2 + is\Gamma_Z/M_Z$ with running Z-boson decay width and $Z_{fi}(s,t)$ is the normalization correction for the Z-boson propagator. $v_i(s,t)$ and $v_f(s,t)$ are modified vector couplings

$$v_i(s,t) = T_{3i} - 2Q_i s_W^2 K_i(s,t), \qquad v_f(s,t) = T_{3f} - 2Q_f s_W^2 K_f(s,t), \tag{11}$$

where T_3 is the third component of the fermion weak isospin. In Eq. (10), the factor $V_{fi}(s,t)$ includes the terms:

$$V_{fi}(s,t) = \Gamma_{vp}(s) + \left(\frac{g_Z}{e}\right)^2 s_W^4 Z_{fi}(s,t) \times \frac{s}{d(s)}[K_{fi}(s,t) - K_f(s,t)K_i(s,t)], \quad (12)$$

where $\Gamma_{vp}(s)$ includes resummed vacuum-polarization loop contributions to the photon propagator, and the complex EW form factors $K_i(s,t)$, $K_f(s,t)$ and $K_{fi}(s,t)$ are defined in Ref. [17].

Equation (10) represents improved photon exchange amplitude with running QED constant and improved Z-boson exchange which include:

(i) Corrections to the photon propagator coming from the vacuum-polarization loops.
(ii) Corrections to the Z-boson propagator and couplings embedded in the form factors $Z_{fi}(s,t)$, $K_i(s,t), K_f(s,t)$ and $K_{fi}(s,t)$.
(iii) Contributions from the WW and ZZ box diagrams also included in the form factors.
(iv) Mixed $\mathcal{O}(\alpha\alpha_s, \alpha\alpha_s^2, \ldots)$ corrections originating from gluon insertions in the self-energy loop diagrams.

The EW form-factor corrections are available in Dizet library [25]. For further details we refer to Ref. [17]. Note that corrections in IBA become numerically sizable at high energies, well above Z-boson peak. At the lower energies one can use the amplitude in which all the form factors and $\Gamma_{vp}(s)$ are replaced by 1.

Next we add the amplitude due to the dipole form factors of the τ lepton, introduced in (3) and (7). Using identities (8) and (9), one obtains

$$\mathcal{M}^{\rm DM} = \frac{e^2 Q_f Q_i}{s} V_{fi}(s,t)\gamma_\mu \otimes \left[A\gamma^\mu + \frac{(p_+ - p_-)^\mu}{2m}(A - iB\gamma_5)\right] + \left(\frac{g_Z}{2}\right)^2 \frac{Z_{fi}(s,t)}{d(s)}\gamma_\mu[v_i(s,t) - a_i\gamma_5] \otimes \left[X\gamma^\mu + \frac{(p_+ - p_-)^\mu}{2m}(X - iY\gamma_5)\right], \quad (13)$$

and the total amplitude is $\mathcal{M} = \mathcal{M}^{\rm IBA} + \mathcal{M}^{\rm DM}$.

2. Spin-correlation matrix

We consider production of the polarized τ^- and τ^+ leptons, which are characterized by the following polarization 3-vectors in their rest-frames, respectively:

$$\vec{s}^- = (s_1^-, s_2^-, s_3^-), \qquad \vec{s}^+ = (s_1^+, s_2^+, s_3^+), \quad (14)$$

where the Cartesian components are defined with respect to the chosen frame. For convenience, we also use unity as the fourth components of the spin vectors:

$$s^- = (s_1^-, s_2^-, s_3^-, 1), \qquad s^+ = (s_1^+, s_2^+, s_3^+, 1). \quad (15)$$

The square of the matrix element averaged over all the polarization states of the initial fermions can be written as

$$|\mathcal{M}|^2 = |\mathcal{M}_\gamma|^2 + |\mathcal{M}_Z|^2 + 2{\rm Re}(\mathcal{M}_\gamma^* \mathcal{M}_Z), \quad (16)$$

which determines the differential cross section taking into account the spin degrees of freedom of the τ leptons as

$$\frac{d\sigma}{d\Omega}(f\bar{f} \to \tau^-\tau^+) = \frac{\beta}{64\pi^2 s}|\mathcal{M}|^2 = \frac{\beta}{64\pi^2 s}\sum_{i,j=1}^{4} R_{i,j} s_i^- s_j^+, \quad (17)$$

where $R_{i,j}$ is explained below.

We rewrite Eq. (17) in the following more convenient form:

$$\frac{d\sigma}{d\Omega}(f\bar{f} \to \tau^-\tau^+) = \frac{d\sigma}{d\Omega}(f\bar{f} \to \tau^-\tau^+)\Big|_{\rm unpol} \times \frac{1}{4}\left(1 + \sum_{i=1}^{3} r_{i,4} s_i^- + \sum_{j=1}^{3} r_{4,j} s_j^+ + \sum_{i,j=1}^{3} r_{i,j} s_i^- s_j^+\right). \quad (18)$$

The elements of spin-correlation matrix $r_{i,j} \equiv R_{i,j}/R_{44}$ and the τ^-, τ^+ polarization states are respectively $r_{i,4} \equiv R_{i,4}/R_{44}$, $r_{4,j} \equiv R_{4,j}/R_{44}$, where $i, j \le 3$.

The cross section for unpolarized τ's is expressed through R_{44}:

$$\frac{d\sigma}{d\Omega}(f\bar{f} \to \tau^-\tau^+)\Big|_{\rm unpol} = \frac{\beta}{16\pi^2 s} R_{44}. \quad (19)$$

If τ decays are taken into account, the vectors defining τ^- and τ^+ density matrices, s_i^- and s_j^+ in Eq. (18), are replaced respectively by the polarimetric vectors, depending on the τ-decay matrix elements, h_i^- and h_j^+.

Furthermore, each contribution in $R_{i,j}$ can be broken down as

$$R_{i,j} = R_{i,j}^{(\gamma)} + R_{i,j}^{(Z)} + R_{i,j}^{(\gamma Z)}, \quad (20)$$

where $R_{i,j}^{(\gamma)}$, $R_{i,j}^{(Z)}$ and $R_{i,j}^{(\gamma Z)}$ represent contributions due to γ exchange, Z-boson exchange and γZ interference, respectively. In the following, we include only terms linear in the dipole form factors. The quantization of $\tau^\mp$ are performed in their respective rest frames. These frames differ from the reaction frame, defined by Eq. (2), by the boosts along $\tau^\mp$ directions.

For energies below and around Z-boson peak, we show results with radiative corrections switched off, as they can be there safely neglected (incorporated into the redefinition of constants). For higher energies, the phenomenological picture would be far more complicated also because of experimental detection/reconstruction criteria, and possibly initial state bremsstrahlung photons of $p_T \sim m_\tau$ getting lost in the beam pipe. That is why, this regime remains out of scope of the present work.[3]

Let us start by recalling results of Ref. [11] for $R^{(\gamma)}_{i,j}$ in case of $e^-e^+ \to \tau^-\tau^+$ process, extended now to also include quarks in the initial state:

$$
\begin{aligned}
R^{(\gamma)}_{11} &= \frac{e^4 Q_i^2}{4\gamma^2 N_i}[4\gamma^2 \mathrm{Re}(A(s)) + \gamma^2 + 1]\sin^2(\theta), & R^{(\gamma)}_{12} &= -R^{(\gamma)}_{21} = \frac{e^4 Q_i^2}{2N_i}\beta \sin^2(\theta)\mathrm{Re}(B(s)),\\
R^{(\gamma)}_{13} &= R^{(\gamma)}_{31} = \frac{e^4 Q_i^2}{4\gamma N_i}[(\gamma^2+1)\mathrm{Re}(A(s)) + 1]\sin(2\theta), & R^{(\gamma)}_{22} &= -\frac{e^4 Q_i^2}{4N_i}\beta^2 \sin^2(\theta),\\
R^{(\gamma)}_{23} &= -R^{(\gamma)}_{32} = -\frac{e^4 Q_i^2}{4N_i}\beta\gamma \sin(2\theta)\mathrm{Re}(B(s)), & R^{(\gamma)}_{33} &= \frac{e^4 Q_i^2}{4\gamma^2 N_i}\{[4\gamma^2 \mathrm{Re}(A(s)) + \gamma^2 + 1]\cos^2(\theta) + \beta^2\gamma^2\},\\
R^{(\gamma)}_{14} &= -R^{(\gamma)}_{41} = \frac{e^4 Q_i^2}{4N_i}\beta\gamma \sin(2\theta)\mathrm{Im}(B(s)), & R^{(\gamma)}_{24} &= R^{(\gamma)}_{42} = \frac{e^4 Q_i^2}{4N_i}\beta^2\gamma \sin(2\theta)\mathrm{Im}(A(s)),\\
R^{(\gamma)}_{34} &= -R^{(\gamma)}_{43} = -\frac{e^4 Q_i^2}{2N_i}\beta \sin^2(\theta)\mathrm{Im}(B(s)), & R^{(\gamma)}_{44} &= \frac{e^4 Q_i^2}{4\gamma^2 N_i}[4\gamma^2 \mathrm{Re}(A(s)) + \beta^2\gamma^2\cos^2(\theta) + \gamma^2 + 1].
\end{aligned}
\tag{21}
$$

The color factor N_i in Eq. (21) is equal to $N_c = 3$ and $N_i = 1$ for the $q\bar{q}$ and e^-e^+ initial state, respectively, while $\gamma = \sqrt{s}/(2m_\tau)$ denotes the Lorentz factor.

Next, we extend the results of Ref. [11] taking into account the Z-boson exchange. Let us start with the component $R^{(Z)}_{i,j}$ that takes into account only the contribution due to the Z-boson exchange, and is the most significant contribution in the vicinity of the Z-peak. This contribution is calculated in terms of the τ-lepton Lorentz factor γ, the velocity β, and the angle θ between the momenta of incoming f_i and τ^- lepton. We express the square of the modulus of the Z-boson propagator as

$$D_Z(s) = (s - M_Z^2)^2 + M_Z^2\Gamma_Z^2, \tag{22}$$

where M_Z and Γ_Z are the mass and decay width of the Z-boson, respectively, and obtain:

$$
\begin{aligned}
R^{(Z)}_{11} &= \frac{g_Z^4 m^4 \gamma^2}{4N_i D_Z(s)}\sin^2(\theta)\{(1-\gamma^2)a_\tau^2 + v_\tau[4\gamma^2\mathrm{Re}(X(s)) + (1+\gamma^2)v_\tau]\}(a_i^2 + v_i^2),\\
R^{(Z)}_{12} &= -\frac{g_Z^4 m^4 \beta\gamma^4}{2N_i D_Z(s)}\sin^2(\theta)[\mathrm{Im}(X(s))a_\tau - \mathrm{Re}(Y(s))v_\tau](a_i^2 + v_i^2),\\
R^{(Z)}_{22} &= \frac{g_Z^4 m^4 \gamma^2}{4N_i D_Z(s)}(\gamma^2-1)\sin^2(\theta)(a_\tau^2 - v_\tau^2)(a_i^2 + v_i^2),\\
R^{(Z)}_{13} &= \frac{g_Z^4 m^4 \gamma^3}{4N_i D_Z(s)}\{4\beta\sin(\theta)a_i[\gamma^2\mathrm{Re}(X(s))a_\tau + (-\gamma^2\mathrm{Im}(Y(s)) + a_\tau)v_\tau]v_i\\
&\quad + \sin(2\theta)[(1-\gamma^2)\mathrm{Im}(Y(s))a_\tau + v_\tau((1+\gamma^2)\mathrm{Re}(X(s)) + v_\tau)](a_i^2 + v_i^2)\},\\
R^{(Z)}_{23} &= -\frac{g_Z^4 m^4 \gamma^3}{2N_i D_Z(s)}\sin(\theta)\{\beta\gamma^2\mathrm{Re}(Y(s))[v_\tau\cos(\theta)(a_i^2 + v_i^2) + 2\beta a_\tau a_i v_i]\\
&\quad + \mathrm{Im}(X(s))[2(-1+\gamma^2)a_i v_\tau v_i + \beta\gamma^2\cos(\theta)a_\tau(a_i^2 + v_i^2)]\},
\end{aligned}
$$

[3]Note that in contrary to Belle II energies or c.m. energy corresponding to the Z peak, at higher energies presence of initial state photons of p_T comparable or higher than the tau mass and at the same time lost in the beam-pipe are not disfavored. This complicates construction of useful for our purposes observables. At the Z-peak energies, such photons are disfavored because then amplitudes are not resonant. At low energies, the ratio of tau mass to beam energy is much larger than the detector minimal acceptance angle.

$$
\begin{aligned}
R_{33}^{(Z)} &= \frac{g_Z^4 m^4 \gamma^2}{8N_i D_Z(s)}\{16\beta\gamma^2\cos(\theta)a_\tau a_i v_\tau v_i + (\gamma^2-1)(3+\cos(2\theta))a_\tau^2(a_i^2+v_i^2)\\
&\quad + (-1+3\gamma^2+(1+\gamma^2)\cos(2\theta))v_\tau^2(a_i^2+v_i^2) + 8\gamma^2\cos(\theta)\mathrm{Re}(X(s))[v_\tau\cos(\theta)(a_i^2+v_i^2)+2\beta a_\tau a_i v_i]\},\\
R_{14}^{(Z)} &= \frac{g_Z^4 m^4 \gamma^3}{2N_i D_Z(s)}\sin(\theta)\{\mathrm{Im}(Y(s))[\beta\gamma^2 v_\tau\cos(\theta)(a_i^2+v_i^2)+2(\gamma^2-1)a_\tau a_i v_i] - v_\tau(2a_i v_\tau v_i+\beta\cos(\theta)a_\tau(a_i^2+v_i^2))\\
&\quad - \mathrm{Re}(X(s))[2(1+\gamma^2)a_i v_\tau v_i+\beta\gamma^2\cos(\theta)a_\tau(a_i^2+v_i^2)]\},\\
R_{24}^{(Z)} &= \frac{g_Z^4 m^4 \gamma^3}{2N_i D_Z(s)}\sin(\theta)\{\mathrm{Im}(X(s))[(\gamma^2-1)v_\tau\cos(\theta)(a_i^2+v_i^2)+2\beta\gamma^2 a_\tau a_i v_i]\\
&\quad + \mathrm{Re}(Y(s))[2\beta\gamma^2 a_i v_\tau v_i+(\gamma^2-1)\cos(\theta)a_\tau(a_i^2+v_i^2)]\},\\
R_{34}^{(Z)} &= \frac{g_Z^4 m^4 \gamma^2}{4N_i D_Z(s)}\{-4a_i v_i\cos(\theta)((\gamma^2-1)a_\tau^2+\gamma^2 v_\tau^2) - \beta\gamma^2(3+\cos(2\theta))a_\tau v_\tau(a_i^2+v_i^2)\\
&\quad - \gamma^2[2\beta\mathrm{Im}(Y(s))\sin^2(\theta)v_\tau(a_i^2+v_i^2)+\mathrm{Re}(X(s))(8\cos(\theta)a_i v_\tau v_i+\beta(3+\cos(2\theta))a_\tau(a_i^2+v_i^2))]\},\\
R_{44}^{(Z)} &= \frac{g_Z^4 m^4 \gamma^2}{8N_i D_Z(s)}\{16\beta\gamma^2\cos(\theta)a_\tau a_i v_\tau v_i + (\gamma^2-1)(3+\cos(2\theta))a_\tau^2(a_i^2+v_i^2) + (1+3\gamma^2+(\gamma^2-1)\cos(2\theta))v_\tau^2(a_i^2+v_i^2)\\
&\quad + 8\gamma^2\mathrm{Re}(X(s))[a_i^2 v_\tau + 2\beta\cos(\theta)a_\tau a_i v_i + v_\tau v_i^2]\},
\end{aligned}
\tag{23}
$$

and the remaining components can be obtained using

$$
R_{j,i}^{(Z)} = R_{i,j}^{(Z)}|_{X(s)\to X(s),Y(s)\to -Y(s)} \quad \text{for } i\neq j. \tag{24}
$$

If only the e^-e^+ initial state is considered, Eq. (23) can be simplified. It simplifies further if one takes into account that the vector coupling for the leptons $v_\tau \approx -0.038$ is numerically quite small. Here, we will keep only the terms linear in v_τ, but neglect the terms $v_\tau X(M_Z^2)$ and $v_\tau Y(M_Z^2)$. Using these approximations, we obtain for the Z-boson contribution [for brevity we denote below $X\equiv X(M_Z^2)$ and $Y\equiv Y(M_Z^2)$] at the energy corresponding to the Z-boson peak:

$$
\begin{aligned}
R_{11}^{(Z)} &= -R_{22}^{(Z)} = -\frac{g_Z^4 a_\tau^4\beta^2 M_Z^2}{64\Gamma_Z^2}\sin^2(\theta),\\
R_{12}^{(Z)} &= R_{21}^{(Z)} = -\frac{g_Z^4 a_\tau^3\beta M_Z^2}{32\Gamma_Z^2}\sin^2(\theta)\mathrm{Im}(X),\\
R_{13}^{(Z)} &= -R_{31}^{(Z)} = -\frac{g_Z^4 a_\tau^3\beta^2 M_Z^2}{64\Gamma_Z^2}\gamma\sin(2\theta)\mathrm{Im}(Y),\\
R_{23}^{(Z)} &= R_{32}^{(Z)} = -\frac{g_Z^4 a_\tau^3\beta M_Z^2}{64\Gamma_Z^2}\gamma\sin(2\theta)\mathrm{Im}(X),\\
R_{14}^{(Z)} &= R_{41}^{(Z)} = -\frac{g_Z^4 a_\tau^3\beta M_Z^2}{64\Gamma_Z^2}\gamma\sin(2\theta)[\mathrm{Re}(X)+v_\tau\gamma^{-2}],\\
R_{24}^{(Z)} &= -R_{42}^{(Z)} = \frac{g_Z^4 a_\tau^3\beta^2 M_Z^2}{64\Gamma_Z^2}\gamma\sin(2\theta)\mathrm{Re}(Y),\\
R_{34}^{(Z)} &= R_{43}^{(Z)} = -\frac{g_Z^4 a_\tau^3\beta M_Z^2}{32\Gamma_Z^2}\{(1+\cos^2(\theta))[v_\tau+\mathrm{Re}(X)]\\
&\qquad + 2v_\tau\beta\cos(\theta)\},\\
R_{44}^{(Z)} &= R_{33}^{(Z)} = \frac{g_Z^4 a_\tau^4\beta^2 M_Z^2}{64\Gamma_Z^2}(1+\cos^2(\theta)),
\end{aligned}
\tag{25}
$$

where $\gamma = M_Z/(2m_\tau)\approx 25.7$ and $\beta\approx 1$.

Finally, let us present the contribution from γZ interference. Close to the Z-peak, and using the same approximations as above, we obtain for the case of incoming e^-e^+ [for brevity we denote below $A\equiv A(M_Z^2)$ and $B\equiv B(M_Z^2)$]:

$$
\begin{aligned}
R_{11}^{(\gamma Z)} &= R_{22}^{(\gamma Z)} = 0,\\
R_{12}^{(\gamma Z)} &= -\frac{e^2 g_Z^2\beta a_\tau v_\tau M_Z}{8\Gamma_Z}\sin^2(\theta),\\
R_{13}^{(\gamma Z)} &= \frac{e^2 g_Z^2 a_\tau\beta M_Z}{8\Gamma_Z}\gamma\sin(\theta)[\mathrm{Re}(Y)-a_\tau\mathrm{Im}(A)],\\
R_{23}^{(\gamma Z)} &= \frac{e^2 g_Z^2 a_\tau\beta M_Z}{8\Gamma_Z}\gamma\sin(\theta)[\beta\mathrm{Re}(X)+a_\tau\beta\mathrm{Im}(B)\\
&\qquad - v_\tau\gamma^{-2}\cos(\theta)],\\
R_{14}^{(\gamma Z)} &= \frac{e^2 g_Z^2 a_\tau M_Z}{8\Gamma_Z}\gamma\sin(\theta)[a_\tau\beta^2\mathrm{Re}(B)-(1+\gamma^{-2})\mathrm{Im}(X)],\\
R_{24}^{(\gamma Z)} &= \frac{e^2 g_Z^2 a_\tau\beta M_Z}{8\Gamma_Z}\gamma\sin(\theta)[\mathrm{Im}(Y)+a_\tau(\gamma^{-2}+\mathrm{Re}(A)],\\
R_{34}^{(\gamma Z)} &= -\frac{e^2 g_Z^2 a_\tau M_Z}{4\Gamma_Z}\cos(\theta)\mathrm{Im}(X),\\
R_{33}^{(\gamma Z)} &= R_{44}^{(\gamma Z)} = -\frac{e^2 g_Z^2 a_\tau^2\beta M_Z}{4\Gamma_Z}\cos(\theta)\mathrm{Im}(A),
\end{aligned}
\tag{26}
$$

and the remaining components can be obtained using

$$
R_{j,i}^{(\gamma Z)} = R_{i,j}^{(\gamma Z)}|_{X\to X,Y\to -Y,A\to A,B\to -B} \quad \text{for } i\neq j. \tag{27}
$$

It is important to identify the components of the matrix $R_{i,j}^{(Z)}$ which are the most sensitive to the weak dipole

moments of τ lepton. Several observations can be made at this point;

(i) The terms $R_{13}^{(Z)}, R_{23}^{(Z)}, R_{14}^{(Z)}, R_{24}^{(Z)}$ in Eq. (25) are enhanced due to the large Lorentz factor γ.

(ii) The τ transverse polarization in the reaction plane along the $\hat{x}$ axis is sensitive to real part of X. The normal to the reaction plane polarization along the $\hat{y}$ axis is sensitive to real part of Y. And finally, the transverse-longitudinal spin correlation $\hat{x}\hat{z}$ and the normal-to-reaction-plane-longitudinal $\hat{y}\hat{z}$ spin correlation depend on the imaginary parts of the weak dipole moments. Thus, it may be possible to construct observables sensitive to particular spin components of the τ leptons.

(iii) We should also note that the interference terms described in Eq. (26) are smaller than the Z-boson contributions by a factor of $\Gamma_Z/M_Z \approx 0.03$, and therefore do not change the dominant pattern.

(iv) Finally, the longitudinal polarization $\mathcal{P}_L = r_{34/43}$ of the τ^- and τ^+ in the SM arises due to the vector coupling v_τ. This is well-known and $\mathcal{P}_L$ was measured already at LEP I, as noted in Ref. [31]. The longitudinal polarization, as can be seen from Eq. (25), depends on the weak anomalous magnetic moment $\mathrm{Re}(X)$ as well.

One can also conclude that the observable studied in Ref. [11], acoplanarity angle between the planes spanned by the τ-lepton decay products, is not sensitive to the weak dipole moments at the Z-peak. This is because at the Z-boson peak, other elements of the matrix $R_{i,j}$ rather than the ones contributing significantly at the Belle II energy of 10.58 GeV [11] start to become dominant.

We would like to acknowledge that in case of $e^-e^+ \to \tau^-\tau^+$ process, the terms linear in the spins and dipole moments were already derived in Refs. [22,30]. However, our results represent some important extensions; they are obtained for various initial-state fermions $i = (e, u, d)$, include the complete spin-correlation matrix between the decaying τ^- and τ^+ leptons, and also include Z-boson exchange, γ^* exchange and $\gamma^* Z$ interference.

B. The $f_i f_i \to \tau^-\tau^+$, $i = \gamma$ case

In the description of the reaction $\gamma(k_1) + \gamma(k_2) \to \tau^-(p_-) + \tau^+(p_+)$ with the on-shell photons ($k_1^2 = k_2^2 = 0$), we separate the contribution of NP from the total SM contribution to $A(0)$ as described in Ref. [9],

$$A(0)_{\mathrm{SM}} = 1.17721(5) \times 10^{-3}, \tag{28}$$

and then define

$$A(0) = A(0)_{\mathrm{SM}} + A(0)_{NP}, \qquad B(0) = B(0)_{NP}. \tag{29}$$

We assume that for the on-shell photons, the dipole moments are real-valued.[4]

The matrix element of this reaction is of the order e^2 and can be written in terms of spinors of the τ leptons as

$$\mathcal{M} = \varepsilon_\mu(k_1)\varepsilon_\nu(k_2)\bar{u}(p_-)\left[\Gamma_\gamma^\mu(k_1)\frac{\not{p}_- - \not{k}_1 + m_\tau}{t - m_\tau^2}\Gamma_\gamma^\nu(k_2) + \Gamma_\gamma^\nu(k_2)\frac{\not{p}_- - \not{k}_2 + m_\tau}{u - m_\tau^2}\Gamma_\gamma^\mu(k_1)\right]v(p_+), \tag{30}$$

where $t = (p_- - k_1)^2$, $u = (p_- - k_2)^2$. The four-vectors of the photon polarization, $\varepsilon_\mu(k_1)$ and $\varepsilon_\nu(k_2)$, obey the conditions $\varepsilon(k_1)\cdot k_1 = \varepsilon(k_2)\cdot k_2 = 0$.

After squaring the matrix element, and averaging over the polarizations of the photons, we obtain

$$|\mathcal{M}|^2 = R_{44}^{\gamma\gamma} + \sum_{i,j=1}^{3} R_{i,j}^{\gamma\gamma} s_i^- s_j^+. \tag{31}$$

The elements of the spin-correlation matrix $R_{i,j}^{\gamma\gamma}/R_{44}^{\gamma\gamma}$ depend on the invariant mass of $\tau^-\tau^+$ pair $s = m_{\tau^-\tau^+}^2$ and the scattering angle θ. Here, we keep only terms linear in the dipole moments.

The expressions for the spin-correlation matrix are presented in terms of the Lorentz factor $\gamma = \sqrt{s}/(2m_\tau)$ of the $\tau^\pm$ leptons, the velocity β and the angle θ.

We define the factor

$$D \equiv 1 - \beta^2\cos^2\theta. \tag{32}$$

The elements of the matrix $R_{i,j}^{\gamma\gamma}$ and $R_{44}^{\gamma\gamma}$ are (for brevity we denote below $A \equiv A(0)$ and $B \equiv B(0)$):

$$R_{11}^{\gamma\gamma} = \frac{e^4}{8D^2}\left[-\beta^2(\beta^2 - 4A - 2)\cos(4\theta) + 4\beta^2(\beta^2 - 2)\cos(2\theta) + 4A(7\beta^2 - 8) - 11\beta^4 + 22\beta^2 - 8\right],$$

$$R_{12}^{\gamma\gamma} = -R_{21}^{\gamma\gamma} = \frac{e^4 B}{4D^2}\beta(\beta^2\cos(4\theta) + 4\cos(2\theta) + 15\beta^2 - 20),$$

[4]We neglect the higher-order contribution to dipole moments coming from the three-photon intermediate state [32], which gives rise to imaginary part of form factors at $q^2 = 0$.

$$
\begin{aligned}
R^{\gamma\gamma}_{13} &= R^{\gamma\gamma}_{31} = \frac{e^4}{2D^2}\gamma\beta^2[(\beta^2 + A(\beta^2-2) - 1)\cos(2\theta) + A\beta^2 - \beta^2 + 1]\sin(2\theta),\\
R^{\gamma\gamma}_{22} &= \frac{e^4}{8D^2}[-\beta^4\cos(4\theta) + 4\beta^2(\beta^2 + 4A)\cos(2\theta) + 16A(\beta^2-2) - 11\beta^4 + 16\beta^2 - 8],\\
R^{\gamma\gamma}_{23} &= -R^{\gamma\gamma}_{32} = \frac{e^4 B}{2D^2}\gamma\beta(\beta^2\cos(2\theta) - 3\beta^2 + 2)\sin(2\theta),\\
R^{\gamma\gamma}_{33} &= \frac{e^4}{8D^2}[\beta^2(\beta^2 - 4A - 2)\cos(4\theta) - 4\beta^4\cos(2\theta) + 4A(9\beta^2 - 8) + 11\beta^4 + 2\beta^2 - 8],\\
R^{\gamma\gamma}_{44} &= \frac{e^4}{8D^2}[-\beta^4\cos(4\theta) + 4\beta^2(\beta^2 - 4A - 2)\cos(2\theta) - 16A(\beta^2-2) - 11\beta^4 + 8\beta^2 + 8].
\end{aligned}
\tag{33}
$$

All elements of $R^{\gamma\gamma}_{i,j}$, except the transverse-longitudinal ones, satisfy the condition $R^{\gamma\gamma}_{i,j}(\theta) = R^{\gamma\gamma}_{i,j}(\pi-\theta)$ for $0 \le \theta \le \pi$.

Note that the contribution from electric dipole moment B is completely separated from the rest of the terms and reads

$$
\begin{aligned}
|\mathcal{M}|^2_{\mathrm{EDM}} = \frac{e^4}{4D^2}\beta B[&(s_1^- s_2^+ - s_2^- s_1^+)(\beta^2\cos(4\theta) + 4\cos(2\theta) + 15\beta^2 - 20)\\
&+ 2(s_2^- s_3^+ - s_3^- s_2^+)\gamma(\beta^2\cos(2\theta) - 3\beta^2 + 2)\sin(2\theta)].
\end{aligned}
\tag{34}
$$

This can be convenient for studying observables sensitive to B.

Finally, the cross section for the process $\gamma\gamma \to \tau^-\tau^+$ is

$$
\begin{aligned}
&\frac{d\sigma}{d\Omega}(\gamma\gamma \to \tau^-\tau^+)\\
&\quad = \frac{d\sigma}{d\Omega}(\gamma\gamma \to \tau^-\tau^+)\Big|_{\mathrm{unpol}} \frac{1}{4}\left(1 + \sum_{i,j=1}^{3} r^{\gamma\gamma}_{i,j} s_i^- s_j^+\right)
\end{aligned}
\tag{35}
$$

with spin correlation matrix $r^{\gamma\gamma}_{i,j} \equiv R^{\gamma\gamma}_{i,j}/R^{\gamma\gamma}_{44}$ and unpolarized cross section

$$
\frac{d\sigma}{d\Omega}(\gamma\gamma \to \tau^-\tau^+)\Big|_{\mathrm{unpol}} = \frac{\beta}{16\pi^2 s} R^{\gamma\gamma}_{44}. \tag{36}
$$

Note that neither the longitudinal nor the transverse τ polarization is present for $\gamma\gamma \to \tau^-\tau^+$. Thus, $r^{\gamma\gamma}_{i,4} = r^{\gamma\gamma}_{4,j} = 0$, and only the spin-correlation part survives in Eq. (35).

III. TRANSVERSE SPIN CORRELATIONS OF ELEMENTARY PROCESSES

In this section, we present numerical results for $R_{i,j}$ for the process $f_i\bar{f}_i \to \tau^-\tau^+$ obtained with analytical formulas of Sec. II, as a function of the invariant mass of τ-lepton pair.

In Figs. 1 and 2, we show $r_{11} = R_{11}/R_{44}$ and $r_{22} = R_{22}/R_{44}$ without including form factors $A(s)$, $B(s)$, $X(s)$ and $Y(s)$, respectively for e^-e^+ and $q\bar{q}$ initial state and two values of scattering angle $\theta = \pi/3$ and $2\pi/3$.

We also used distributions from Fig. 1 to test our formulas with respect to the predictions of KKMC, including a test of the frame conventions. The plots of other elements $r_{i,j}$ are not as interesting, because they are very small (except for the τ mass effects), and therefore are not shown.

The pattern of the transverse spin correlations, r_{11} and r_{22}, is mostly dominated by the SM correlations, and is not straightforward to explain. It depends on the flavor and scattering angle, and as a consequence, in case of $q\bar{q}$ initial state, it is parton distribution function (PDF) dependent. The electron-positron case is more straightforward in terms of definition of a suitable observable, as the incoming state is always e^-e^+.

The transverse spin correlations for e^-e^+ and $u\bar{u}$ change signs twice, at energies below and above the Z peak, and then for higher energies stabilize at small positive value, except for e^-e^+ at $\theta = 2\pi/3$, where value is larger. This is not the case for $d\bar{d}$ initial state, where correlations change sign only once below Z-boson peak, and then remain negative and small (large) for $\theta = \pi/3$ ($\theta = 2\pi/3$). Above the Z-boson peak, they only very weakly depend on energy.

In addition, in Fig. 1 (lower plots) we show dipole form factors impact on the R_{44} which determines the cross section of $e^-e^+ \to \tau^-\tau^+$ of unpolarized τ leptons. The ratios of R_{44} calculated with the form factors $\mathrm{Re}(A(s))$ and $\mathrm{Re}(X(s))$ included, to $R_{44}(SM)$ calculated without form factors, are presented. As is seen, there is a clear effect of the real parts of anomalous magnetic and anomalous weak magnetic form factors. The electric form factors $B(s)$ and $Y(s)$ do not contribute to R_{44}, while the contribution from $\mathrm{Im}(A(s))$ and $\mathrm{Im}(X(s))$ is very small and is not shown.

In Fig. 3, we show $R^{\gamma\gamma}_{44}$ and other elements $r^{\gamma\gamma}_{i,j}$ for the process $\gamma\gamma \to \tau^-\tau^+$ with and without dipole moments included. The chosen values of dipole moments $A(0) = 0.1$ and $B(0) = 0.1$ are perhaps unrealistically large, but allow

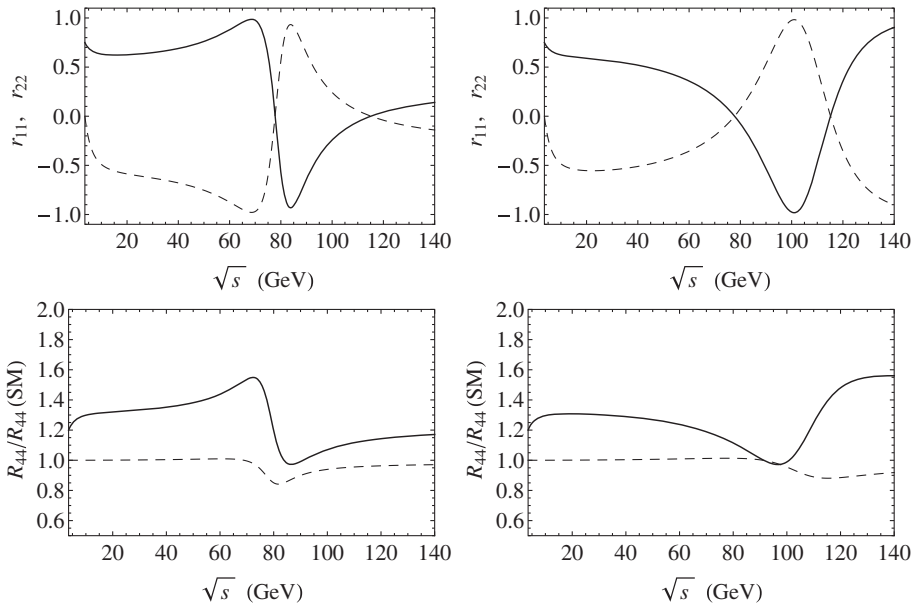

FIG. 1. Upper plots: transverse spin-correlation elements of the $r_{i,j}$ matrix; r_{11} (solid lines) and r_{22} (dashed lines) for the electron-positron initial state. The angle θ is chosen $\pi/3$ for the left plot and $2\pi/3$ for the right plot. The effective Z couplings to leptons of Table II are used. Dipole moments are not included. Lower plots: $R_{44}/R_{44}(SM)$ at $\theta = \pi/3$ (left), and $\theta = 2\pi/3$ (right). Solid lines: $\mathrm{Re}(A(s)) = 0.1$, dashed lines: $\mathrm{Re}(X(s)) = 0.1$, other form factors are set to zero.

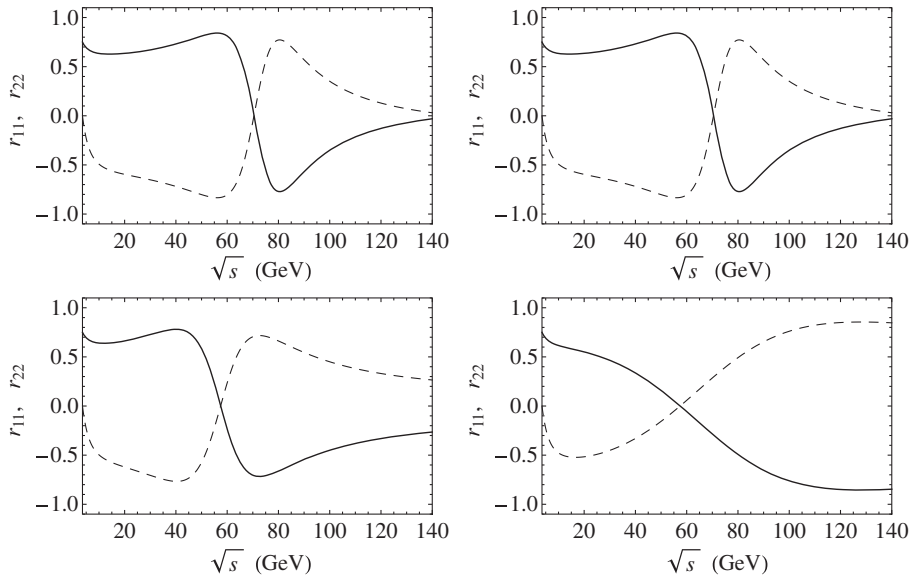

FIG. 2. Transverse spin-correlation components r_{11} (solid lines) and r_{22} (dashed lines) for the $u\bar{u}$ (top plots) and $d\bar{d}$ (bottom plots) initial states. The angle θ of quark vs τ^- is chosen $\pi/3$ in the left plots and $2\pi/3$ in the right plots. The effective couplings of Z to quarks from Table II are used. Dipole moments are not included.

us to demonstrate the sensitivity of various elements to the dipole moments. In particular, one can observe that the elements $r_{12}^{\gamma\gamma}$ and $r_{23}^{\gamma\gamma}$ vanish in the absence of the electric dipole moment, and become finite for nonzero values of it, while the other elements depend only on the anomalous magnetic dipole moment.

IV. REWEIGHTING PROCEDURE

The analytical formulas presented in Sec. II have been implemented into reweighting algorithms for KKMC and TauSpinner programs. Necessary tests were performed to confirm that event weights at fixed τ-pair virtuality and incoming fermion flavors reproduce those formulas correctly.

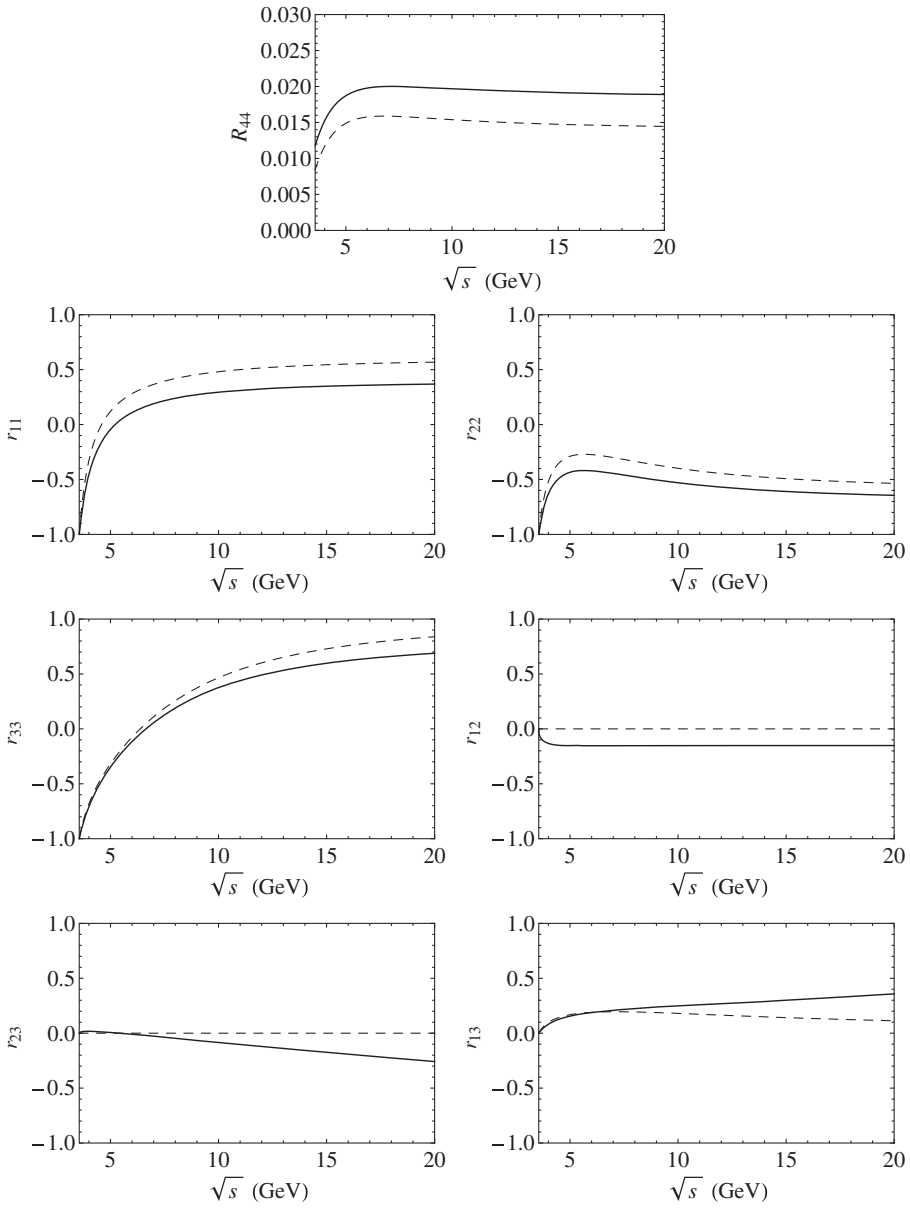

FIG. 3. Energy dependence of $R_{44}^{\gamma\gamma}$ and $r_{i,j}^{\gamma\gamma}$. Solid lines are calculated for the values $A = 0.1$ and $B = 0.1$; dashed lines—for $A = B = 0$. The angle θ is chosen $\pi/3$.

A. The reweighting algorithm for KKMC: Case of anomalous dipole moments

With respect to implementation prepared in Ref. [11], the function calculating the spin correlations and an overall event weight has been updated to include contributions due to Z-boson exchange and $Z\gamma$-interference contributions. The formulas have become substantially longer after introducing the anomalous couplings of the τ leptons to the Z-bosons along with coupling to the virtual photons. Other technical aspects explained in Ref. [11] remain valid.

However, for higher energies the p_T of the intermediate boson can become larger than m_τ because of more frequent initial-state bremsstrahlung. Thus, the validity tests of improved Born approximation for constructing the event weight should be repeated. The usage of the reference frames as described in Refs. [18,33] may be needed. This is true both for e^-e^+ and pp applications, as discussed in the following section. We will return to this point in a future work, when important details of planned experiments become available and impact of bremsstrahlung on the analysis procedure can be quantified.

Another minor detail that also has been improved in the present version of the code is an explicit rotation by angle π around the y-axis, which is necessary to match the reference frame used in our present formulas and in the KKMC code.

B. The reweighting algorithm for TauSpinner

The basic formalism of TauSpinner is documented in Eqs. (7)–(12) in Sec. 2.2 of Ref. [34]. Here we assume that reader is familiar with this reference, and on the details of how the kinematics of hard process can be deciphered from the information available in the event record.

Let us briefly recall the basic equation used in the reweighting algorithm,

$$d\sigma = \sum_{\text{flavors}} dx_1 dx_2 f(x_1,\ldots) f(x_2,\ldots) d\Omega^{\text{parton level}}_{\text{prod}} d\Omega_{\tau^+} d\Omega_{\tau^-} \times \left(\sum_{\lambda_1,\lambda_2} |\mathcal{M}^{\text{prod}}_{\text{parton level}}|^2\right)\left(\sum_{\lambda_1} |\mathcal{M}^{\tau^+}|^2\right) \times \left(\sum_{\lambda_2} |\mathcal{M}^{\tau^-}|^2\right) wt_{\text{spin}}, \tag{37}$$

which represents product of phase-space integration elements and matrix elements, squared and averaged over spin. Sum over flavors of incoming partons and integration over PDFs is also given. Let us provide some details. The sum over flavors is followed by integration elements over incoming partons energy fractions and PDFs. Then, the Lorentz invariant phase-space integration elements at the parton level to τ-pair production and for the decay of τ^+ and τ^- follow. Terms in brackets correspond to spin-averaged matrix elements for τ production and each τ decay respectively. The sum over τ-decay channels is not given explicitly. Only the spin weight

$$wt_{\text{spin}} = \sum_{i,j=t,x,y,z} r_{i,j} h^i_{\tau^+} h^j_{\tau^-} \tag{38}$$

depends on kinematics of both $\tau^\pm$ production and decay in a rather simple way, as explained below. It is a smooth function, which in addition satisfies the conditions $\langle wt_{\text{spin}}\rangle = 1$ and $0 < wt_{\text{spin}} < 4$.

In Eq. (38), $h^i_{\tau^+}$ and $h^j_{\tau^-}$ denote the polarimetric vectors, which for a particular τ^+ or τ^- decay channel depend on the kinematics of $\tau^\pm$ decays. The $r_{i,j}$ matrix combining each τ spin-polarization and τ-pair spin-correlation matrix depends on the τ-production kinematic (including incoming parton flavors) only.

For reweighting, the ratio of expressions given by Eq. (37) is calculated for two distinct assumptions of the matrix elements. Obviously, the phase-space integration elements cancel out in the ratio. For the sums, several rather trivial options are possible. In particular, they depend on which terms in the matrix element used in the event sample generation differs from the one used in the variant to be implemented.

In this update, starting with the $q\bar{q} \to \tau^-\tau^+$ parton-level processes, the functions calculating the spin correlations and an overall event weight have been updated in the TauSpinner with analytical formulas of Sec. II. Before this update, the transverse spin correlations in the process $q\bar{q} \to Z/\gamma^* \to \tau^-\tau^+$ were available via the EW library SANC [28,35] and its predefined tables, which were neither very flexible nor transparent.

Next, let us turn our attention to the new parton level process, $\gamma\gamma \to \tau^-\tau^+$. The formulas for spin amplitudes, cross section and spin-correlation matrix were presented in Sec. II. Equation (33) contain all necessary expressions. It is important to note that each parton process contributes incoherently to the final state. Thus, the introduction of nearly on shell photon as an incoming parton, and a corresponding hard process, is possible by straightforward extension of the sums in Eq. (37) only.

For the set of PDFs, we can take the ones described in Refs. [36,37]. These structure functions include the photon PDF as well, but this choice may be not straightforward. The actual choice may depend on the details of the selection criteria of the heavy-ion collision events. In some cases, the contribution from the γ PDFs may even dominate, and the usually large Drell-Yan contributions may become relatively small.

In terms of technical details of the TauSpinner, we again assume that the reader is familiar with the ones described in Ref. [34]. Minor extensions to include additional parton-level $\gamma\gamma$ process has been introduced in this update.[5]

Three new functions have been added to the TauSpinner code, and the sum in function `double sigborn(...)` was extended to the $\gamma\gamma$ process. In the function `dipolgammarij(...)`, we calculate the $R^{\gamma\gamma}_{i,j}$ matrix. The functions `T_gamm(MODE,SVAR,COSTHE,TA,TB)` and `T_gammNEW(MODE,SVAR,COSTHE,TA,TB)` calculate cross section normalized as in older parton level processes; anomalous dipole moments are absent in `T_gamm()`. The function `T_gamm` can be set to return zero with internal parameters of the algorithm. This feature is useful for reweighting samples which have no $\gamma\gamma$ contribution. The functions `T_gamm` and `T_gammNEW` are called by the algorithm with input parameters named `MODE, SVAR, COSTHE, TA,` and `TB`, respectively. The `MODE` is not used at present. The Mandelstam s variable `SVAR`, cosine of the hard process scattering angle `COSTHE` and helicities/chiralities `TA`, and `TB` of the outgoing τ's are set internally based on the event kinematics, and are not expected to be initialized by the user.

The `T_gamm` function does not depend on anomalous moments, which are introduced via call to `T_gammNEW` only, and subsequent call to `dipolgammarij`. The

[5]Practical comments can be found in the code of the latest version of Tauspinner, downloadable from the project web page http://tauolapp.web.cern.ch/tauolapp/.

parameters (constants) which require initialization by the user in the appropriate `struct` or common blocks are

(i) `IFgammOLD`: allows to switch $\gamma\gamma$ contribution on/off in weight denominator according to what is present in generated sample.
(ii) `Adip`: anomalous magnetic moment.
(iii) `Bdip`: anomalous electric moment.
(iv) `iqed=iqedDip`: to include SM magnetic dipole moment in $\gamma\gamma$ contribution in the denominator of the ratio defining weight, see Eqs. (19) and (20) of Ref. [11]. The choice depends on whether the contribution is taken into account in the sample to be reweighted. Note that this contribution is always present in the weight in the numerator, unless the photon-structure function is absent (set to zero).

The implementation of the initializations parameters currently hard coded in routine `T_gamm` is not universal. The actual choice of parameters can be generalized following discussions with interested users.

As is the case with all parton-level processes of Eq. (37) presented in Ref. [34], the $\gamma\gamma$ functions `T_gamm` and `T_gammNEW` provide results with τ leptons helicity-level approximation. The transverse spin correlations are not included at this step in the algorithm. Complete spin correlations are introduced later in the algorithm step while calculating and using $wt_{\rm spin}$. From now, in the loop over summation used to calculate the averaged $R_{i,j}$ matrix on the basis of Eq. (37), contributions of $R_{i,j}$ from $\gamma\gamma$, Eq. (33), are introduced.

The implementation can be adapted for reweighting events of ultraperipheral heavy ions collisions, where it can be used for the analyses of τ dipole moments at LHC, as done in the Refs. [5,6].

V. NUMERICAL RESULTS FOR SEMIREALISTIC OBSERVABLE

In Ref. [11], we discussed the observables sensitive to contribution of the dipole form factors in the $e^-e^+ \to \gamma^* \to \tau^-\tau^+$ interaction at Belle II energies. We found that transverse spin correlations of the τ-pair production, combined with $\tau^\pm \to \pi^\pm\pi^0\nu_\tau$ decays, may be useful for that purpose. For these energies, the transverse spin correlations, calculated at the lowest order in the SM are simple, and weakly dependent on the c.m. energy. Transverse spin correlations in the direction perpendicular to (aligned in) the reaction plane are of the opposite sign. Therefore, fortunately the corresponding kinematic configurations are easy to separate, and the initial-state bremsstrahlung (ISR) emissions do not contribute in sizable amounts to the transverse momenta of the $e^-e^+ \to \tau^-\tau^+ n\gamma$ events. The transverse momenta of unobservable photons $p_T^{\rm ISR}$ are much smaller than m_τ and, as a consequence, also smaller than the transverse momenta of the τ-decay products.

A. Observables sensitive to dipole moments at the Z-boson pole

At the Z-boson peak, the spin-correlation pattern is different from that at low energies relevant for the Belle II experiments. The largest components of the R matrix are of longitudinal-transverse type, e.g. the terms R_{13}, R_{31}, R_{23}, and R_{32} are large. That is why the observable of Ref. [11] is not sensitive to the anomalous magnetic and electric dipole form factors.

We have chosen therefore different and also rather simple observable, for the case when both τ leptons decay to a π and a ν_τ. In the center of mass of $\tau^-\tau^+$ pair, we take the energy to correspond to the mass of Z-boson. That should, in realistic conditions, reduce the size of the initial-state bremsstrahlung, even though the width of the Z-boson is larger than the mass of the τ-lepton. This aspect will require large care and detailed understanding of detector conditions in the future experiments at the Future Circular Collider (FCC-ee) at the Z-boson peak.

We calculate vector products of the particle momenta

$$\vec{v}_1 = \vec{p} \times \vec{k}, \qquad \vec{v}_2 = \vec{p}_{\pi^-} \times \vec{p}_{\nu_\tau}, \qquad \vec{v}_3 = \vec{p} \times \vec{v}_1, \quad (39)$$

and normalize these three-vectors to the unit length; $\hat{v}_i = \vec{v}_i/|\vec{v}_i|$ $(i = 1, 2, 3)$. Here $\vec{p}_{\pi^-}$ and $\vec{p}_{\nu_\tau}$ are the momenta of π^- and ν_τ coming from the decay $\tau^- \to \pi^-\nu_\tau$. Then the acoplanarity angle between the plane spanned on the vectors $\vec{k}$ and $\vec{p}$, and the plane spanned on the vectors $\vec{p}_{\pi^-}$ and $\vec{p}_{\nu_\tau}$, is determined from the relations

$$\cos(\varphi) = \hat{v}_1 \cdot \hat{v}_2, \qquad \sin(\varphi) = \hat{v}_2 \cdot \hat{v}_3. \quad (40)$$

This acoplanarity angle spans the range from 0 to 2π.

The number of events with and without dipole moments included vs acoplanarity angle is calculated for the energy, corresponding to the Z-boson peak $\sqrt{s} = M_Z = 91.1876$ GeV. In these conditions the Z exchange plays the dominant role, and the γZ interference gives a minor contribution. Therefore it becomes possible to investigate effect of the weak dipole moments $X(M_Z^2)$ and $Y(M_Z^2)$. It is rather clear from Eq. (25) that the dominant dipole moment contributions $R_{13}^{(Z)}, R_{23}^{(Z)}, R_{14}^{(Z)}, R_{24}^{(Z)}$ are proportional to $\cos(\theta)$ and therefore would vanish if integrated over the whole region of θ. However, assuming that the τ momenta are reconstructed, we can select the forward or backward ranges of the angle θ, and thus, obtain sensitivity to the dipole moments. Results of the calculations are presented in Fig. 4.

As it is seen from Fig. 4 (top), the real part of $X(M_Z^2)$ and $Y(M_Z^2)$ generate, respectively, the event distribution $\sim 1 + 0.008\cos(\varphi)$ and $\sim 1 - 0.008\sin(\varphi)$. As pointed in Sec. II A in discussion of Eq. (25), these observables are chosen to be sensitive to the transverse and normal to the reaction-plane τ spin degree of freedom.

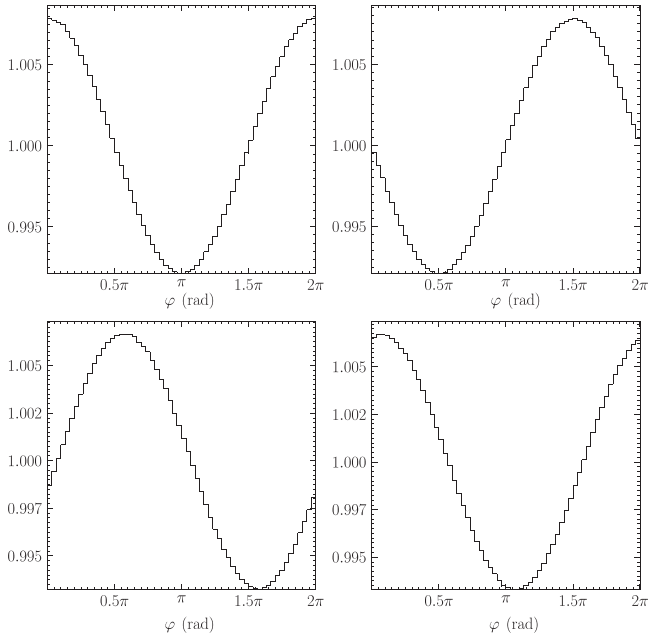

FIG. 4. Ratio of number of events with and without weak dipole moments included, as a function of the acoplanarity angle φ at the energy $\sqrt{s} = M_Z$. The backward angles θ are selected, i.e. $\cos(\theta) < 0$. The top left plot is calculated for $\mathrm{Re}(X) = 0.0004$, the top right plot is calculated for $\mathrm{Re}(Y) = 0.0004$, the bottom left is calculated for $\mathrm{Im}(X) = 0.0004$, and the bottom right is calculated for $\mathrm{Im}(Y) = 0.0004$. For the imaginary form factors, the constraint $E_{\pi^+} > E_{\bar{\nu}_\tau}$ is applied on the τ^+ side. The magnetic and electric form factors $A(M_Z^2) = B(M_Z^2) = 0$ are used.

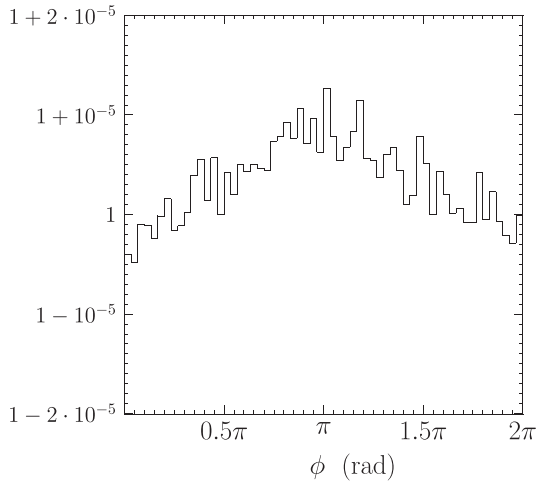

FIG. 5. Impact of Z-exchange to the acoplanarity of $\pi^\pm\pi^0$ planes of $\tau^\pm$ decay products. The production process $e^+e^- \to \tau^+\tau^- n\gamma$, and decays $\tau^\pm \to \pi^\pm\pi^0\nu_\tau$ at the center-of-mass energy 10.58 GeV are used. Events are selected so that there is the same sign of energy differences for the charged and neutral pions coming from decays $\tau^- \to \pi^-\pi^0\nu_\tau$ and $\tau^+ \to \pi^+\pi^0\bar{\nu}_\tau$. The detailed definition of presented observable is given in Ref. [11]. The ratio of the acoplanarity distributions with and without Z-boson contribution is shown.

The imaginary parts of $X(M_Z^2)$ and $Y(M_Z^2)$ result in the event distributions shown in Fig. 4 (bottom). Since they involve transverse-longitudinal, R_{13}, and normal-to-reaction-plane-longitudinal, R_{23}, spin correlations, these distributions appear sensitive to dipole moments only if the longitudinal component of the momentum of π^+, which comes from the $\tau^+ \to \pi^+\bar{\nu}_\tau$ decay, is constrained. To increase the magnitude of the distributions, we impose the condition $E_{\pi^+} > E_{\bar{\nu}_\tau}$ on the energies of π^+ and $\bar{\nu}_\tau$.

As one can see, the imaginary part of $X(M_Z^2)$ and of $Y(M_Z^2)$ generates, respectively, the distribution $\sim 1 + 0.008\sin(\varphi - \delta)$ and $\sim 1 + 0.008\cos(\varphi - \delta')$ with small shifts δ and δ'. These shifts are caused by non-dominant spin-correlation coefficients, for example, by $R_{12}^{(Z)}$, which slightly modifies distribution for $\mathrm{Im}(X(M_Z^2))$.

The magnitude of the weak-dipole moment effects in all distributions is about 0.008. This may seem too large in view of the chosen very small value 0.0004 of the dipole moments. The observed enhancement is due to the large Lorentz factor at the Z peak.

B. The effect of Z-boson exchange at Belle II energy

Let us turn our attention to lower energies. In Ref. [11], we studied effects of the dipole form factors, $A(s)$ and $B(s)$, on spin effects and on an observable of potential interest for the Belle II measurement. Since this is expected to be a precision measurement, that is why the effect of Z-boson exchange, or better to say the $Z - \gamma^*$ interference, which could represent potential bias, should be addressed. In Fig. 5, we present the ratio of distributions where the Z-boson contribution is turned on or off. The distributions are prepared exactly in the same manner as for Fig. 2 of Ref. [11]. The $\tau^\pm \to \pi^\pm\pi^0\nu_\tau$ decay channels are used for the production process $e^-e^+ \to \tau^-\tau^+ n\gamma$ at Belle II energy. Acoplanarity between the planes spanned by the $\pi^-\pi^0$ system (from τ^-) and the $\pi^+\pi^0$ system (from τ^+), respectively, is monitored. The momenta are boosted to the rest frame of visible decay product system of $\pi^-\pi^0\pi^+\pi^0$ mesons. An additional selection criteria on the pions energies, $(E_{\pi^-} - E_{\pi^0})(E_{\pi^+} - E_{\pi^0})$ to be larger or smaller than zero, is applied.

The anomalous magnetic and electric form factors are not taken into account. We see that the bias on the spin-observable sensitive to dipole moments due to Z-contributions is at the level of 10^{-5}. Thus, the effect of Z-boson exchange can be considered to give a rather small correction even when analyzing $> 10^{10}$ events that are expected to be collected at the Belle II experiment. We can conclude that the observable of Ref. [11] remains useful for studying the magnetic and electric dipole form factors at the Belle II energies.

On the other hand, we find that the observable of Ref. [11] does not have much sensitivity to the dipole moments for higher energies, of the Z-boson peak. In this

case, an alternative observable is needed, possibly the one presented in the previous subsection.

C. The case of pp collisions

Constructing observable sensitive to dipole moments in the pp collisions is far more difficult. The signatures of anomalous dipole moments in $\gamma\gamma$ parton level collision can not be separated from parton processes of $q\bar{q}$ collisions. Also, contrary to the e^+e^- case, the choice of the direction of the $\hat{z}$ axis in the reference frame to be used can be ambiguous. Finally, defining the p_T of the hard reaction system does not seem to be straightforward.

In $\gamma\gamma \to \tau\tau$ process, the largest sensitivity to the dipole moments come from $R^{\gamma\gamma}_{13}, R^{\gamma\gamma}_{31}$ and $R^{\gamma\gamma}_{23}, R^{\gamma\gamma}_{32}$ elements of $R^{\gamma\gamma}_{i,j}$ matrix. This imply that our choice of the τ decays could be $\tau^\pm \to \pi^\pm \nu_\tau$ and $\tau^\mp \to \pi^\mp \pi^0 \nu_\tau$. The observable could be the difference of the $\pi^\pm$ energy spectra in subsamples defined by whether difference of the $\pi^\mp$ and π^0 momenta tend to be closer to reaction plane or outside. The backgrounds, e.g. the Drell-Yan quark-level processes, do not have large transverse-longitudinal R-matrix components. At low virtualities, the SM contribution to Drell-Yan $R^{(\gamma)}_{23/32}$ is zero, and in the relativistic limit $R^{(\gamma)}_{13/31}$ is nondominant. Also in peripheral collisions, the contribution from the Drell-Yan should be reduced. This impact of spin correlations on dipole-moment phenomenology offers an interesting starting point for further work with more details of hadron collider conditions taken into account.

VI. SUMMARY AND OUTLOOK

In this paper, we have discussed effects from electric and anomalous magnetic dipole moments of the τ leptons on transverse spin correlations in the τ-pair production and decay.

These studies include calculation of the analytical formulas for spin-amplitude components and spin-correlations matrices, for $e^-e^+ \to \tau^-\tau^+$, $q\bar{q} \to \tau^-\tau^+$ and $\gamma\gamma \to \tau^-\tau^+$ processes. In case of the s-channel $f_i\bar{f}_i \to \tau^-\tau^+$ process, including photon and Z-boson exchange, their interference and radiative corrections in framework of IBA, makes those formulas applicable for a large range of τ-pair invariant mass, from the Belle II energies up to above WW and ZZ pair-production thresholds. Numerical predictions for the ratios of transverse components of spin-correlations matrices were also shown and discussed.

The analytical formulas are embedded into algorithms for generated events reweighting, to be used with KKMC generator for events produced in e^-e^+ collisions and TauSpinner program for pp collisions.

To demonstrate applications of the reweighting algorithm, semirealistic observables are suggested, and for e^-e^+ case numerical results are presented for anomalous dipole moments at high energies and for Z-boson exchange contribution to Belle II energies.

A. Technical developments

The algorithm for the implementation of anomalous magnetic and electric dipole moments for the s-channel photon exchange in $e^+e^- \to \tau^+\tau^-$ process was enriched with contribution of Z-boson exchange. With the help of the extension to include Z-boson contributions, the impact on dipole moment observable ambiguities at Belle II energies can be studied. The algorithm can be used also for higher energies in its present form up to and above the ZZ-boson pair-production threshold. At these energies, contributions from WW- and ZZ-boson pair production become double resonant and box-diagram contributions become sizable. Their impact on spin effects cannot be neglected.

The observable, acoplanarity of decay products of τ-lepton pairs, survive upgrade to high energies after minor modifications, provided the effects of photon radiation can be ignored, as in the case of $\sqrt{s} \simeq M_Z^2$. We have checked the results for a new observable, and also with the help of analytic calculations. We conclude that tools for further studies of more experimental details are prepared. It is again an add-up to KKMC and may be useful not only for the FCC oriented studies, but also for the evaluation of potential biases in the Belle II precision measurements as well.

We prepared and installed in TauSpinner a preliminary version of the code necessary for including $\gamma\gamma \to \tau^-\tau^+$ parton-level process in event reweighting. It can be added with or without including anomalous dipole moments. We have also enriched implementation of event weight for $q\bar{q} \to \tau^-\tau^+$ process with the possibility to study impact of anomalous dipole moments on transverse spin correlations.

There is important issue about the QCD and EW corrections; those corrections have been extensively studied, for example, in Refs. [38–41], in which progress in automated calculation of matrix elements has been achieved. Of course, for precise SM simulation of the τ-pair production, these higher-order corrections need to be taken into account. In the present paper, these corrections are included in framework of improved Born approximation [17,25].

Also the effects of multiparton interactions [42,43] and underlying events [44–46] may be of importance. Note that in general, evaluations of underlying events and multiparton interaction effects are investigated in the framework of experimental collaboration work. At the same time, experimental details of detection and background subtractions have to be taken into account. Let us stress again that all these efforts are needed to ensure the robustness of the event sample. One can expect reweighting results to be meaningful only if its precision is established

The TauSpinner reweighting algorithm for introduction of new effects is expected to supplement events with rather

small corrections; event weights close to 1. That is why the demand on precision of NP effects is not very strict provided that the predictions of the SM are not compromised. The use of the present paper algorithms may be considered as the first step of the work, as we assume that the impact of interactions resulting with dipole moments will not affect the SM part of the interaction sizably.

B. Outlook

Reliability of reweighting at high energies requires some attention, but as we work for a discovery tool, not a precision tool, that may be postponed to further studies. So far, tests when photon radiation is removed with generation variable cuts were performed only. That is suitable for Belle II applications, but for high energy applications, such as at the FCC, further work on selection cuts to prevent degradation of the performance due to bremsstrahlung is needed. It will require careful future considerations for detector acceptance and more focus on the details of the detector than on tool validation. At the FCC bremsstrahlung photons lost in the beam pipe may have p_T comparable to the τ-lepton mass. That means further studies and program extensions are needed for such configurations. For example, at the c.m. energy around the Z-boson peak presence of such photons is largely reduced. However, the program can now be used for studies with no bremsstrahlung events or events of rather soft photons with energy and/or p_T sizably smaller than half of the τ mass. This is not a constraint for program use at Belle II energies, where bremsstrahlung photons lost in the beam pipe cannot have large p_T. At high energies, the so-called Mustraal frame [33,47,48] for weight calculation may need to be used, as already proposed for evolution of future versions of TauSpinner.

ACKNOWLEDGMENTS

A. Yu. K. acknowledges partial support by the National Academy of Sciences of Ukraine via the program "Participation in the international projects in high-energy and nuclear physics" (Project No. C-4/53-2023). He is grateful to the Polska Akademia Nauk for the financial support during his stay at the Institute of Nuclear Physics PAS. This project was supported in part from funds of Narodowe Centrum Nauki under Decisions No. DEC-2017/27/B/ST2/01391, No. UMO-2022/01/3/ST2/00027, and of the Consortium Polonais des Institutions Nucleaires and Institut National de Physique Nucl'eaire et de Physique des Particules Collaboration with Laboratoire d'Annecy de Physique des Particules - Annecy. This project was supported by the U.S. Department of Energy under research Grant No. DE-SC0022350.

[1] N. F. Ramsey, Electric dipole moments of particles, Annu. Rev. Nucl. Part. Sci. **32**, 211 (1982).
[2] Hai-Yang Cheng, CP violating effects in leptonic systems, Phys. Rev. D **28**, 150 (1983).
[3] W. Bernreuther and O. Nachtmann, CP violating correlations in electron positron annihilation into τ leptons, Phys. Rev. Lett. **63**, 2787 (1989); **64**, 1072(E) (1990).
[4] K. Inami *et al.*, An improved search for the electric dipole moment of the τ lepton, J. High Energy Phys. 04 (2022) 110.
[5] Georges Aad *et al.*, Observation of the $\gamma\gamma \to \tau\tau$ process in $Pb + Pb$ collisions and constraints on the τ-lepton anomalous magnetic moment with the ATLAS detector, Phys. Rev. Lett. **131**, 151802 (2023).
[6] Armen Tumasyan *et al.*, Observation of τ lepton pair production in ultraperipheral lead-lead collisions at $\sqrt{s_{\mathrm{NN}}} = 5.02$ TeV, Phys. Rev. Lett. **131**, 151803 (2023).
[7] B. Abi *et al.*, Measurement of the positive muon anomalous magnetic moment to 0.46 ppm, Phys. Rev. Lett. **126**, 141801 (2021).
[8] W. Bernreuther, A. Brandenburg, and P. Overmann, CP violation beyond the Standard Model and tau pair production in e^+e^- collisions, Phys. Lett. B **391**, 413 (1997); **412**, 425(E) (1997).
[9] S. Eidelman and M. Passera, Theory of the tau lepton anomalous magnetic moment, Mod. Phys. Lett. A **22**, 159 (2007).
[10] Sw. Banerjee, D. Biswas, T. Przedzinski, and Z. Was, The tau lepton Monte Carlo event generation—imprinting new physics models with exotic scalar or vector states into simulation samples, arXiv:2112.07330.
[11] Sw. Banerjee, A. Yu. Korchin, and Z. Was, Spin correlations in τ-lepton pair production due to anomalous magnetic and electric dipole moments, Phys. Rev. D **106**, 113010 (2022).
[12] Christian Bierlich *et al.*, A comprehensive guide to the physics and usage of PYTHIA 8.3, SciPost Phys. Codeb. **2022**, 8 (2022).
[13] Enrico Bothmann *et al.*, Event generation with Sherpa 2.2, SciPost Phys. **7**, 034 (2019).
[14] Z. Czyczula, T. Przedzinski, and Z. Was, TauSpinner program for studies on spin effect in tau production at the LHC, Eur. Phys. J. C **72**, 1988 (2012).
[15] J. Kalinowski, W. Kotlarski, E. Richter-Was, and Z. Was, Production of τ lepton pairs with high p_T jets at the LHC and the TauSpinner reweighting algorithm, Eur. Phys. J. C **76**, 540 (2016).

[16] T. Przedzinski, E. Richter-Was, and Z. Was, TauSpinner: A tool for simulating CP effects in $H \to \tau\tau$ decays at LHC, Eur. Phys. J. C **74**, 3177 (2014).
[17] E. Richter-Was and Z. Was, Documentation of TauSpinner approach for electroweak corrections in LHC $Z \to \ell\ell$ observables, Eur. Phys. J. C **79**, 480 (2019).
[18] E. Richter-Was and Z. Was, Adequacy of effective Born for electroweak effects and TauSpinner algorithms for high energy physics simulated samples, Eur. Phys. J. Plus **137**, 95 (2022).
[19] W. Hollik, Jose I. Illana, S. Rigolin, C. Schappacher, and D. Stockinger, Top dipole form-factors and loop induced CP violation in supersymmetry, Nucl. Phys. **B551**, 3 (1999); **B557**, 407(E) (1999).
[20] R. L. Workman *et al.*, Review of particle physics, Prog. Theor. Exp. Phys. **2022**, 083C01 (2022).
[21] DELPHI Collaboration, Study of tau-pair production in photon-photon collisions at LEP and limits on the anomalous electromagnetic moments of the tau lepton, Eur. Phys. J. C **35**, 159 (2004).
[22] J. Bernabeu, G. A. Gonzalez-Sprinberg, M. Tung, and J. Vidal, The Tau weak magnetic dipole moment, Nucl. Phys. **B436**, 474 (1995).
[23] ALEPH Collaboration, Search for anomalous weak dipole moments of the tau lepton, Eur. Phys. J. C **30**, 291 (2003).
[24] Yasuhiro Yamaguchi and Nodoka Yamanaka, Quark level and hadronic contributions to the electric dipole moment of charged leptons in the Standard Model, Phys. Rev. D **103**, 013001 (2021).
[25] Dmitri Yu. Bardin, P. Christova, M. Jack, L. Kalinovskaya, A. Olchevski, S. Riemann, and T. Riemann, ZFITTER v.6.21: A semianalytical program for fermion pair production in e^+e^- annihilation, Comput. Phys. Commun. **133**, 229 (2001).
[26] J. A. Grifols and A. Mendez, Electromagnetic properties of the tau lepton from Z^0 decay, Phys. Lett. B **255**, 611 (1991); **259**, 512(E) (1991).
[27] Mateusz Dyndal, Mariola Klusek-Gawenda, Matthias Schott, and Antoni Szczurek, Anomalous electromagnetic moments of τ lepton in $\gamma\gamma \to \tau^+\tau^-$ reaction in $Pb + Pb$ collisions at the LHC, Phys. Lett. B **809**, 135682 (2020).
[28] A. Arbuzov, S. Jadach, Z. Was, B. F. L. Ward, and S. A. Yost, The Monte Carlo program KKMC for the lepton or quark pair production at LEP/SLC energies—updates of electroweak calculations, Comput. Phys. Commun. **260**, 107734 (2021).
[29] V. B. Berestetskii, E. M. Lifshitz, and L. P. Pitaevskii, *Quantum Electrodynamics*, Volume 4 of Course of Theoretical Physics (Pergamon Press, Oxford, 1982).
[30] J. Bernabeu, G. A. Gonzalez-Sprinberg, and J. Vidal, Normal and transverse single tau polarization at the Z peak, Phys. Lett. B **326**, 168 (1994).
[31] J. Mnich, Experimental tests of the standard model in $e^+e^- \to f$ anti-f at the Z resonance, Phys. Rep. **271**, 181 (1996).
[32] Werner Bernreuther, Long Chen, and Otto Nachtmann, Probing the tau electric dipole moment at the BEPC-II collider, Phys. Rev. D **104**, 115002 (2021).
[33] E. Richter-Was and Z. Was, Separating electroweak and strong interactions in Drell–Yan processes at LHC: Leptons angular distributions and reference frames, Eur. Phys. J. C **76**, 473 (2016).
[34] T. Przedzinski, E. Richter-Was, and Z. Was, Documentation of TauSpinner algorithms: Program for simulating spin effects in τ-lepton production at LHC, Eur. Phys. J. C **79**, 91 (2019).
[35] A. Andonov, A. Arbuzov, D. Bardin, S. Bondarenko, P. Christova, L. Kalinovskaya, G. Nanava, and W. von Schlippe, SANCscope—v.1.00, Comput. Phys. Commun. **174**, 481 (2006); **177**, 623(E) (2007).
[36] Spencer R. Klein, Joakim Nystrand, Janet Seger, Yuri Gorbunov, and Joey Butterworth, STARlight: A Monte Carlo simulation program for ultra-peripheral collisions of relativistic ions, Comput. Phys. Commun. **212**, 258 (2017).
[37] Keping Xie, T. J. Hobbs, Tie-Jiun Hou, Carl Schmidt, Mengshi Yan, and C. P. Yuan, Photon PDF within the CT18 global analysis, Phys. Rev. D **105**, 054006 (2022).
[38] J. Alwall, R. Frederix, S. Frixione, V. Hirschi, F. Maltoni, O. Mattelaer, H. S. Shao, T. Stelzer, P. Torrielli, and M. Zaro, The automated computation of tree-level and next-to-leading order differential cross sections, and their matching to parton shower simulations, J. High Energy Phys. 07 (2014) 079.
[39] R. Frederix, S. Frixione, V. Hirschi, D. Pagani, H. S. Shao, and M. Zaro, The automation of next-to-leading order electroweak calculations, J. High Energy Phys. 07 (2018) 185; 11 (2021) 85(E).
[40] Celine Degrande, Claude Duhr, Benjamin Fuks, David Grellscheid, Olivier Mattelaer, and Thomas Reiter, UFO—The Universal FeynRules Output, Comput. Phys. Commun. **183**, 1201 (2012).
[41] Luc Darmé *et al.*, UFO 2.0: The 'Universal Feynman Output' format, Eur. Phys. J. C **83**, 631 (2023).
[42] Stefan Gieseke, Christian A. Rohr, and Andrzej Siodmok, Tuning of the multiple parton interaction model in Herwig++ using early LHC data, in *Proceedings of the 3rd International Workshop on Multiple Partonic Interactions at the LHC, MPI@LHC 2011, Hamburg, Germany, 2011*, edited by S. Platzer and M. Diehl (Deutsches Elektronen-Synchrotron, DESY, Hamburg, 2012), pp. 67–74, 10.3204/DESY-PROC-2012-03.
[43] D. Lincoln, Multiple parton interaction studies at *DØ*, Nucl. Part. Phys. Proc. **273–275**, 2118 (2016).
[44] Vardan Khachatryan *et al.*, Event generator tunes obtained from underlying event and multiparton scattering measurements, Eur. Phys. J. C **76**, 155 (2016).
[45] T. Affolder *et al.*, Charged jet evolution and the underlying event in $p\bar{p}$ collisions at 1.8 TeV, Phys. Rev. D **65**, 092002 (2002).
[46] Georges Aad *et al.*, Measurement of underlying event characteristics using charged particles in pp collisions at $\sqrt{s} = 900$ GeV and 7 TeV with the ATLAS detector, Phys. Rev. D **83**, 112001 (2011).
[47] Frits A. Berends, R. Kleiss, and S. Jadach, Radiative corrections to muon pair and quark pair production in electron-positron collisions in the Z^0 region, Nucl. Phys. **B202**, 63 (1982).
[48] E. Richter-Was and Z. Was, W production at LHC: Lepton angular distributions and reference frames for probing hard QCD, Eur. Phys. J. C **77**, 111 (2017).